Upper Limb Joint Space Modeling of Stroke Induced Synergies Using Isolated and Voluntary Arm Perturbations

Matt Simkins, Aimen H. Al-Refai, *Member, IEEE*, and Jacob Rosen, *Member, IEEE*

***Abstract*—Among other diminished motor capabilities, survivors of a stroke often exhibit joint synergies. These synergies are stereotypically characterized by involuntary joint co-activation. With respect to the upper limbs, such synergies diminish coordination in reaching, pointing, and other daily tasks. The primary goal of this research is to model synergy and quantify it in a comprehensive and mathematically tractable form. A motion capture system was used to measure joint rotations from stroke survivors and control subjects. These data showed that joint synergies are nonunique and asymmetric. The model also provided a way to calculate joint combinations that result in maximum and minimum synergy. Beyond providing a more complete view of synergies, this approach could facilitate new ways to evaluate and treat stroke survivors. In particular, this approach may have applications in diagnostic and treatment algorithms for use in rehabilitation robots.**

***Index Terms*—Rehabilitation, robotic, singular value decomposition (SVD), stroke, synergy.**

I. Introduction

JOINT synergies are one among several effects that diminish coordination of the left or right upper limb following the incidence of stroke [1], [2]. One of the goals of physical therapy is to reduce joint synergies and increase selective voluntary movements [3]. Therefore, objective and quantifiable measures are needed to identify abnormal synergies and to monitor the emergence of voluntary movement during, and following therapy. The terms "joint synergy" and "muscle synergy" are often used in the literature to describe the same type of motor deficit in which joint movements are coupled. In joint synergy, an attempt to move a single joint results in movement of multiple joints. Joint synergy in healthy individuals is sometimes described as a beneficial attribute characterized as the coordinated co-activation of various muscles to accomplish a task [4]. This paper focuses on an altogether different type of synergy that is undesirable. Pathological synergy is defined here as an involuntary phenomenon, resulting from brain damage, that diminishes control.

Upper-limb synergies have certain stereotypical features that are classically divided into "flexor" and "extensor" synergies [5]. Flexor synergy describes mutual coupling between elbow-flexion, shoulder-abduction, shoulder-extension, shoulder-external-rotation, wrist flexion, wrist/elbow-supination, and wrist-ulnar-deviation [6]. Extensor synergy describes coupling in the reverse directions from flexor synergy.

Clinical measures of stroke synergy often rely on subjective examinations. For example, the Fugl–Meyer (FM) assessment uses a three-point scale that is based on a visual assessment of specified multi-joint reaching tasks [7]. While practical and repeatable [6], the FM has a coarse ordinal scoring system that is not suitable for parametric analysis. As researchers continue to evaluate new treatment approaches, there are likely to be slight differences in outcomes between proposed rehabilitation regimes and standard care. Therefore, continual, incremental improvements in therapeutic approaches will require assessment techniques that are more sensitive to improvements in motor control in general, and joint synergy in particular.

Previous research efforts to quantify synergy have focused on static and dynamic measurements for a single joint [8]. In static measurements of synergy the limbs were held in fixed positions and only isometric data were collected [9], [10]. Dynamic measures of synergy have made use of torque measurements with electromyography (EMG). Analogous studies were performed for the lower limbs [11]. With few exceptions [12], multi-joint synergy experiments generally involve pointing or reaching tasks in Cartesian space (task space) [7], [13]–[15].

The overarching goal of the reported study is to develop an objective methodology to assess and quantify joint synergy. The proposed methodology is then tested using an experimental approach with both healthy and stroke subjects. This study differs from previous research efforts in two ways. First, these analyses are based on kinematic data. While torque and/or EMG signal measures have certain advantages, kinematic measures are more practical clinically [15] since clinical assessments of synergy often involve visual observations that are essentially kinematic in nature. Second, the methodology and analysis are conducted in joint space [16] to evaluate all seven degrees-of-freedom in the arm: three shoulder axes, two elbow axes, and two wrist axes. In order to quantify synergy a linear model is used as an approximation [17]. Previous efforts often evaluate synergy by studying end effector trajectories in task space rather than joint rotations in joint space. Given that joint synergies act directly on joints, data collected in Cartesian space offer only indirect measures of synergy.

Manuscript received July 31, 2012; revised January 14, 2013, April 10, 2013, May 22, 2013, and July 10, 2013; accepted July 11, 2013. Date of publication July 31, 2013; date of current version April 28, 2014.

The authors are with the Department of Computer Engineering, University of California at Santa Cruz, Santa Cruz, CA 95064 USA (e-mail: msimkins@ucsc.edu; aalrefai@ucsc.edu; rosen@ucsc.edu).

Digital Object Identifier 10.1109/TNSRE.2013.2273313

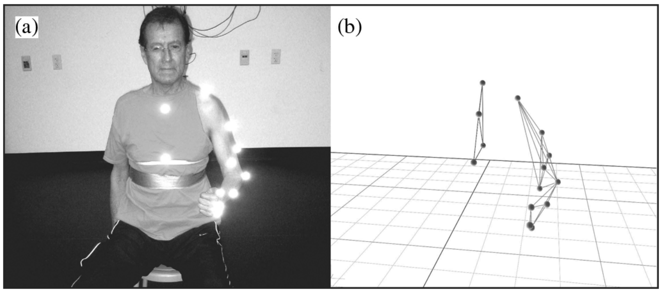

Fig. 1. Experimental setup for a stroke survivor with left-side hemiparesis. Pictured in (a) is the stroke survivor. Makers appear as bright points. Pictured in (b) is the subject-specific arm model. Dots represent marker locations.

II. METHODS

A. Apparatus

Subjects were seated on a metal chair. A strap was used to fixate the subjects' torso to the chair [18]. Fourteen motion capture markers were taped to the thorax and arm of subjects. Marker locations are depicted in Fig. 1. Ten ceiling mounted Vicon MX cameras were pointed at a target volume centered on the subjects' arm. Marker positions were recorded with sub-millimeter accuracy (Vicon Motion Systems, Oxford, U.K.). The camera sampling rates were 100 Hz. Following data acquisition, joint angles were calculated using Vicon Bodybuilder code. Joint angle information was then processed using various MATLAB scripts (Mathworks Inc., Natick, MA, USA).

B. Subjects

Subject data are summarized in Table I. The hemiparetic stroke survivor population covered as large a range of impairment as possible. All stroke survivors were in a chronic phase of recovery. A Modified Fugl-Meyer (MFM) assessment for the upper-limbs was conducted to determine the level of disability. MFM scores ranged from 0 (poor) to 14 (good). Hemiparetic MFM scores are depicted in Fig. 4 of the Results section. Three subjects had received botulinum toxin injections in their effected arm 1–10 years prior to the study. All three subjects reported having no noticeable residual effects from their botulinum toxin treatments. Experimental controls for the cause of brain injuries, (hemorrhagic or ischemic) were deemed unnecessary [19]. Likewise, there were no controls for gender. The hemiparetic population was generally older. Because age was a possible confounding factor [15], five age-matched control subjects were included. All control subjects were neurologically intact. This research was approved by the University of California, Santa Cruz, Internal Review Board. All subjects provided written consent prior to participation.

C. Protocol

The experiment ranged from 60 to 90 min in duration. All arm motions started and ended from approximately the same position, as depicted in Fig. 1. This start/end position is required in the FM for forearm pronation/supination. The FM does include an alternative start position for shoulder flexion and abduction with the elbow fully extended at 0°. A start/end position with the elbow at 90° was selected for all movements in this experiment. Using a single position provided more experimental control. Additionally, the 90° elbow position resulted in better marker visibility. This start/end position also optimized the subjects' arm manipulability [16]. Subjects were asked to slowly and deliberately move their arm, one joint axis at a time, until they had moved all seven joint axes. A more detailed description of each isolated joint movement is given in the "Required Movement" column of Table II. Each iteration through the seven joint axes was considered a set. All subjects completed three sets. The joint axes number assignments, joint axes abbreviations, and required movements, are given in Table II.

TABLE I
SUBJECT DATA

Subject Number	Type	Age [years]	Time Post-Stroke [years]	Sex	Effected Side
1	Stroke Survivors	69	4	Male	Left
2		75	1	Female	Left
3		70	14	Male	Right
4		58	6	Male	Right
5		63	6	Male	Right
6		82	4	Female	Right
7		67	15	Female	Right
8		56	2	Female	Right
9		54	11	Female	Left
10		65	14	Male	Right
11		61	15	Female	Right
12	Non-age-Matched Controls	45	Healthy	Male	Right
13		55	Healthy	Male	Left
14		28	Healthy	Male	Left
15		23	Healthy	Male	Right
16		21	Healthy	Male	Left
17		19	Healthy	Male	Right
18	Age-matched Controls	64	Healthy	Male	Left
19		77	Healthy	Male	Right
20		62	Healthy	Male	Left
21		61	Healthy	Male	Right
22		78	Healthy	Male	Right

For control subjects the "effected side" denotes the subject's dominant limb.

D. Modeling and Data Analysis

Joint synergies are characterized by the involuntary co-activation of joints. As such, if an individual attempted to move one joint, then the existence of synergy requires that one or more other joints will respond. Rotation of other joints is practically inevitable, even in healthy individuals. Involuntary synergies that are evident in neurologically intact subjects are therefore referred to as "natural" synergies.

If the synergistic interactions are assumed to be linear, then the functional relationship between the joint being intentionally moved, x, and the joint that moves in synergy, y, is approximated as follows:

$$y \approx a^* x + b \tag{1}$$

where b relates to the initial start angle. To give an example of how this model relates to a specific synergistic joint interaction, consider wrist flexion synergy in response to voluntary shoulder

TABLE II
JOINT MOVEMENTS

Joint	Axis No.	Positive Rotation	Axis Abbreviation	Required Movement
Elbow	1	Flexion	EF	Extend, flex, and extend to start.
	2	Pronation	EP	Pronate, then supinate to start.
Shoulder	3	Flexion	SF	Flex, then extend to start.
	4	Inner Rotation	SR	Rotate in, out, then in to start.
	5	Abduction	SA	Abduct, then adduct to start.
Wrist	6	Flexion	WF	Flex, then extend to start.
	7	Ulnar Deviation	WU	Ulnar deviate, radial deviate to start.

Pronation and supination are sometimes associated with the wrist rather than the elbow. Both interpretations are equivalent. The relevance of axes numbers are addressed in the Data Analysis Section. The column "required movement" describes how subjects were asked to move during the experiment. Axes descriptions relate to positive rotation for the given joint. For example, a negative value for EF indicates elbow extension rather than flexion.

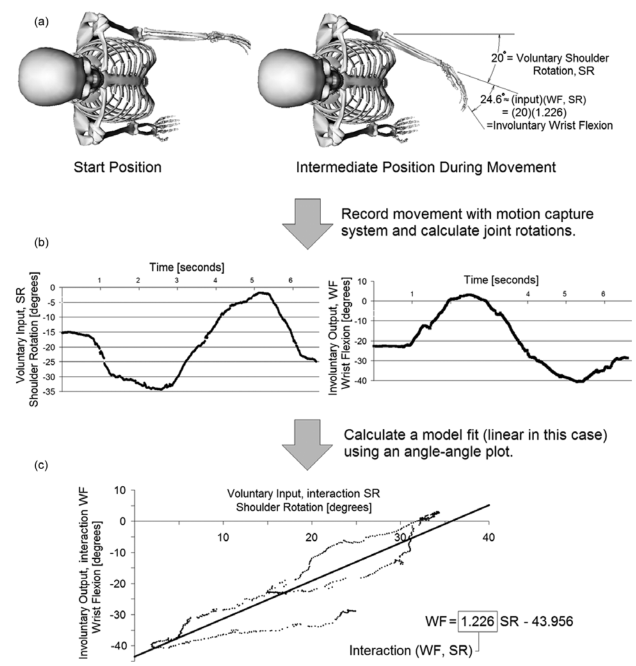

Fig. 2. Process for calculating a single interaction using Subject 2 as the example. Skeletal images were generated on OpenSim 2.4.0 (Stanford University).

inner rotation. For reference, this interaction is depicted graphically in Fig. 2. Assume that a subject is asked to perform isolated shoulder rotation (SR), see Table II. Among the other joints axes, suppose that it is desired to know how much the wrist will synergistically flex (WF). The following linear regression equation is therefore obtained using least squares to describe the interaction

$$y \approx WF = 1.226^{*}SR - 43.956. \tag{2}$$

An important limitation of (1) is that it only describes the synergistic relationship between one pair of joints at a time. However, activities of daily living (ADL) are likely to involve the simultaneous rotation of multiple joints. Therefore, a more useful model of synergistic movement would consider the combined synergistic contributions from multiple joints. To accomplish this, synergies are expressed as a matrix. To help describe the matrix being proposed, assume that the independent variable x_1 represents the angle of voluntary elbow flexion about joint axis 1, x_2 represents voluntary elbow pronation about axis 2, x_3 about axis 3, and so on. Likewise, y_1 represents synergistic elbow flexion, y_2 represents synergistic elbow pronation, and so on. In this way the following model is obtained:

$$\mathbf{y} = \mathbf{A}\mathbf{x} + \mathbf{b} \tag{3}$$

where $\mathbf{x}$ is the vector of intended joint angles and $\mathbf{y}$ is the vector of joint angles that are predicted by the linear model. The elements of $\mathbf{A}$, a_{ij}, relates to the strength of the synergistic interaction between the ith and jth joints. The model in (3) assumes that all arm motions originate from the same start position. Therefore, for $\mathbf{x} = \mathbf{0}$, $\mathbf{b} = \mathbf{y}_0$ where $\mathbf{y}_0$ is the initial joint angles. The focus of this research is on joint interactions. Therefore, $\mathbf{b}$ does not yield particularly meaningful synergy information and is not discussed in detail.

The relationship between the joint that a subject attempts to move and the way that the joint actually moves is difficult, and perhaps impossible to know. For this reason it is taken for granted that the measured response angle for the joint being intentionally rotated is equal to the intended rotation. Therefore, the coefficients of $\mathbf{A}$ are always one along the diagonal. In the case of zero synergy, $\mathbf{A}$ equals the identity matrix.

While it is possible to measure $\mathbf{y}$, the model in $\mathbf{A}$ is unknown without knowledge of a subject's intended motion. To determine this, the columns of $\mathbf{A}$ are estimated experimentally by having the subject move one joint at a time. The rows of $\mathbf{A}$ are then used to predict the synergistic response of the ith joint in $\mathbf{y}$ given some *intended* combination of the other six joint axes.

The model described by (3) is based on kinematic data. Arm dynamics, gravity, forces, and torques are not considered [8]. This model is based on several assumptions. First, a linear relationship is used to model human arm movement. Second, (3) assumes that the same joint relationships apply regardless of the start or end angle. For this reason the start/end positions are not important and we can neglect vector $\mathbf{b}$. Third, (3) assumes that the principle of superposition holds. Therefore, in the strictest sense, this model is most reliably applied to discrete, singular joint movements and it *might* apply to more complex multi-joint movements. Fourth, (3) assumes that each voluntary input angle *uniquely* maps to one, and only one output angle. With respect to synergy, uniqueness means that interactions are the same for flexion as for extension. Conversely, in a "nonunique" interaction the synergistic flexion joint path will differ significantly from the extension joint path. Note, this fourth assumption does not relate to matrix symmetry. The topic of symmetry and uniqueness are addressed further in the Discussion section.

There are two ways to envision synergy. Research on the topic often studies synergistic interaction of specific joints [8], [10]. As an example, this first view might seek to determine how joint EF responds to joint EP. Consistent with this view, the size of the interactions between joints describes the strength of the synergy. In order to summarize the strengths of these synergies across subjects, interactions are reported in terms of root mean squared (rms). Thus, a strong or weak synergistic interaction is reflected by a higher or lower rms value respectively. Data was summarized with rms values for specific interactions as well as for complete matrices. Another way to view synergy is in terms that the therapeutic community often uses. According to this view, synergy is described by the simultaneous rotation of multiple joints. Hence, full arm movements are used to describe flexor or extensor synergies. Therefore, the second view seeks to determine how much the entire arm might move in response to the simultaneous attempt to move joint EF, EP, ... WU. In order to capture the combined synergistic effects of multi-joint motion, singular value decomposition (SVD) is used. Importantly, rms values of synergy only relate indirectly to measures obtained through SVD.

It stands to reason that there exists some combination of joints that exacerbate the effects of synergy more than others. In this way we can define the concepts of maximum and minimum synergy. Maximum synergy is defined as the synergistic response that results in the largest unintended movement. Minimum synergy is defined as the synergistic response that results in the smallest movement compared to what is intended. For the special case of zero synergy with completely independent joint movements (which is practically impossible for normal human movement) maximum and minimum synergy are undefined. Often SVD is used to determine, or reduce matrix dimensionality. However, SVD also provides a way to determine maximum and minimum synergy. A key point is that *minimum synergy is arguably just as undesirable as maximum synergy*. In this context, minimum synergy relates to undesirable synergy effects that are ordinarily not considered. An important distinction for this work is that SVD is not being used to simplify, or change the $\mathbf{A}$ matrix in any way. Instead, SVD is used to evaluate the impact of using right singular vectors as inputs for $\mathbf{x}$. The impact of a right singular vector on arm motion is reflected by the corresponding singular value. SVD was performed on all synergy matrices and these relationships become clearer when the results are presented.

SVD results in the following expression:

$$\mathbf{A} = \mathbf{U}\mathbf{\Sigma}\mathbf{V}^{\mathrm{T}} \tag{4}$$

where $\mathbf{U}$ and $\mathbf{V}$ express the left and right singular vectors and $\mathbf{\Sigma}$ contains singular values along its diagonal. The columns of $\mathbf{V}$ are expressed as $\mathbf{v}_j$ where j is the jth column of $\mathbf{V}$. Singular values in $\mathbf{\Sigma}$ are expressed as σ_j where j is the jth row and column of $\mathbf{\Sigma}$. Singular values are arranged in descending order with $\sigma_1 \geq \sigma_2 \geq \ldots \geq \sigma_7$ such that σ_1 is the maximum, and σ_7 is the minimum singular value. SVD is related to principal component analysis (PCA) and others have used PCA to evaluate synergy [20], [21]. However, PCA was used in a different context in that PCA models were based on variation.

Mathematically, a larger disparity between the maximum and minimum singular values will scale inputs more extremely along principal axes. To use a geometric analogy, dissimilar singular values will stretch a unit disk into an ellipse [22]. Due to this scaling, $\|\hat{\mathbf{y}}\|$ is maximized when $\mathbf{x}$ is proportional to $\mathbf{v}_1$, and is minimized when $\mathbf{x}$ is proportional to $\mathbf{v_7}$ [23]. For this reason, the singular values could be considered an alternative measure of synergy that considers combinations of joints. Plainly stated, $\mathbf{v}_{\mathrm{j}}$ describes which joints, and by how much a person intends move their arm. The singular values, σ_{j}, describes how much that particular joint combination is synergistically scaled.

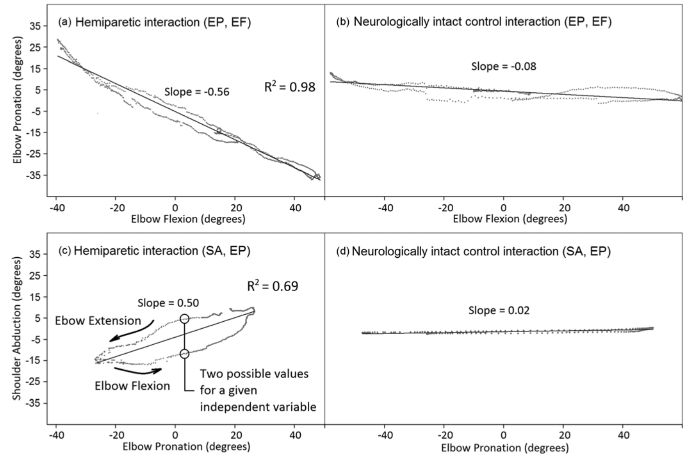

Fig. 3. Approximately unique, and nonunique interactions for hemiparetic subject 1, (a) and (c). Subject 13, a neurologically intact subject, is given in (b) and (d). Dots in the dotted lines represent data points, solid lines are linear least squares fits. The slopes for the linear fits are also given. Axes were scaled and data was shifted (offset) for readability. Therefore, the *shapes* of these data are accurate, but the position relative to the axis is arbitrary.

III. Results

A. Modeling Joint Synergy

The calculation of a single linear interaction, wrist flexion in response to shoulder inner rotation (WF, SR) is depicted in Fig. 2. Fig. 2(a) represents a typical example of postprocessed joint angles, calculated from marker positions, in which a hemiparetic subject has initiated shoulder rotation. The full repetition includes shoulder inner rotation, shoulder external rotation, followed by internal rotation back to the start/stop position. Among the other joints, the subject *involuntarily* flexes their wrist during shoulder inner rotation. Notice that the synergistic wrist response in Fig. 2(a) is scaled by interaction (WF, SR). Fig. 2(b) and (c) show how (WF, SR) is calculated. Only the wrist flexion/shoulder rotation interaction is depicted. In reality, the motion capture system recorded all seven joint axes simultaneously for such movements. Fig. 2(b) depicts the calculated joint angles as a function of time using Vicon Bodybuilder. Finally, Fig. 2(c) depicts a linear model fit.

B. Uniqueness

Formally, the definition of a function requires that an input *uniquely* map to one, and only one output. To varying extents, many interactions were nonunique. To demonstrate this, Fig. 3 shows examples of unique and nonunique interactions. The data in Fig. 3(a) and (c) are from a hemiparetic subject. Notice in (a) that the data points are all relatively close to the fitted line. Accordingly, the residuals are small and the R^2 is 98%, a good fit. A nonunique interaction for the same hemiparetic subject is given in (c). Notice in (c) that the flexion and extension paths are different. Accordingly, the residuals are larger and the R^2 is only 69%. This relationship is clearly nonunique if the model must accommodate two outputs for a single input, one output for extension, and one output for flexion. For perspective, the same two interactions are given for a neurologically intact subject in Fig. 3(b) and (d). As was typical for neurologically intact subjects, the synergy (as measured by the slope) is small and the interaction is mostly flat.

C. Magnitude of Synergistic Interactions for Subjects

Comparing the synergy for a given interaction from two synergy matrices is relatively simple. Each interaction relates to some element in the matrix and the larger elements correspond to the higher synergy. Comparing the overall arm movements of two subjects requires that all interactions be considered collectively. Finding a way to quantify overall synergy from an entire matrix is, to some extent, a matter of interpretation. As was mentioned previously, one way to quantify overall synergy is to take the rms of the off-diagonal interactions (recall that the elements along the diagonals are all equal 1). An rms was calculated for each matrix in this way using (3). Admittedly, information is certainly lost by reducing all of the data contained in a 7×7 matrix to a single number. However, rms calculations provide a convenient way to present summary statistics. A more content rich description of synergy is presented further on when SVD results are considered.

The matrix rms values were consistent with MFM scores in that higher impairments roughly correlated to higher levels of synergy. The scatter plot in Fig. 4 depicts the matrix rms values plotted against the corresponding MFM scores for all hemiparetic subjects. The regression equation in Fig. 4 was

$$\mathrm{rms} = 1.18 - 0.0648^{*}\mathrm{MFM} \qquad (5)$$

with both indicator variables, 1.18 and -0.0648 being significant. Both indicator variables had p-values <0.001. Therefore, (5) demonstrates a significant negative relationship between the MFM scores and matrix rms values.

The matrix rms scores were also able to distinguish hemiparetic subjects from neurologically intact subjects. A one-way ANOVA was performed on the matrix rms calculations for the three groups: hemiparetic, nonage-matched controls, and age-matched controls. The resulting ANOVA p-value was <0.001. This indicates that there was a statistically significant difference for at least one of the three groups. Post hoc pairwise differences for all three groups were then assessed with Tukey's method using a 95% confidence level. Age-matched and nonage-matched means were not significantly different from each other, but they were both significantly different from hemiparetic subjects. Put another way, age was not a significant factor, but the incidence of stroke was a significant factor. Because age-matched and nonage-matched control subjects were not significantly different, the analysis that follows will treat them as a single control group. Furthermore, these results suggest that linear modeling was sufficiently robust to distinguish hemiparetic individuals from neurologically intact individuals.

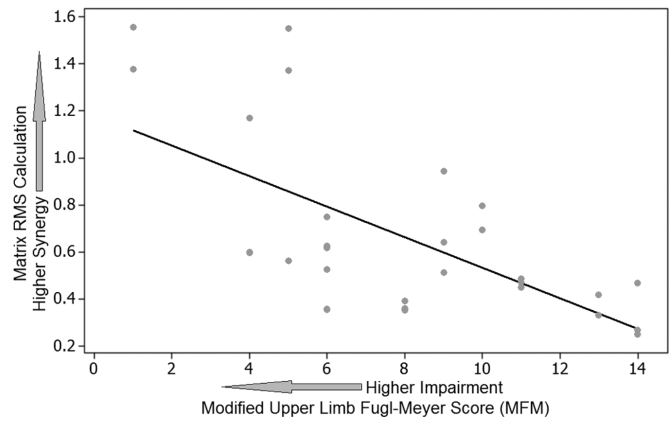

Fig. 4. Scatter plot of MFM scores versus synergy matrix rms values. Lower MFM scores roughly translated to higher matrix rms synergies.

D. Magnitude of Synergistic Interactions for Specific Joints

For studying differences between interactions, rms values across all subjects, for each interaction, are plotted in Fig. 5(a) and (c). The rms values given in Fig. 4 utilized values across *different* interactions in the matrix. However, the rms calculations in Fig. 5 are across subjects for the *same* interaction. Mean values with 95% confidence intervals (CIs) for those interactions are plotted on bottom, in (b) and (d). The intent of plotting the CI and rms values together is to graphically summarize the interaction magnitudes as well as the interaction sign consistencies across subjects. rms values are always positive. However, taking the average of negative and positive interactions moves the overall mean closer to zero. High variation of interactions also expands the CI. Thus, rms is an indication of how strong a given interaction is while the CI and mean indicate how consistent the interaction was across subjects.

While there are known stereotypical synergies, there existed significant differences among stroke survivors. Several strong hemiparetic interactions with large rms values had low mean values and larger CIs. Thus, in some cases hemiparetic subjects had a significant number of positive and negative synergies for the same interaction. Black filled bars distinguish several instances of such interactions in Fig. 5(a). Notice that the CIs are relatively large and the mean values are small for interactions (SA, SF), (EP, SR), and (SR, SF) in Fig. 5(b) even though the rms values in (a) are relatively large.

These data do not indicate that stroke induced synergies are necessarily a magnification of the natural synergies found in controls. This is evident by comparing the sequence of interactions between hemiparetic and control subjects in Fig. 5. If the effects of stroke were simply a magnification of existing natural synergies then one would expect the same ordering of interactions in Fig. 5(a) and (c). However, with the exception of interaction (WF, SR), the orderings are very different.

The synergetic joint interactions, as expressed by the synergy matrix, were asymmetric. For clarity, the therapy community

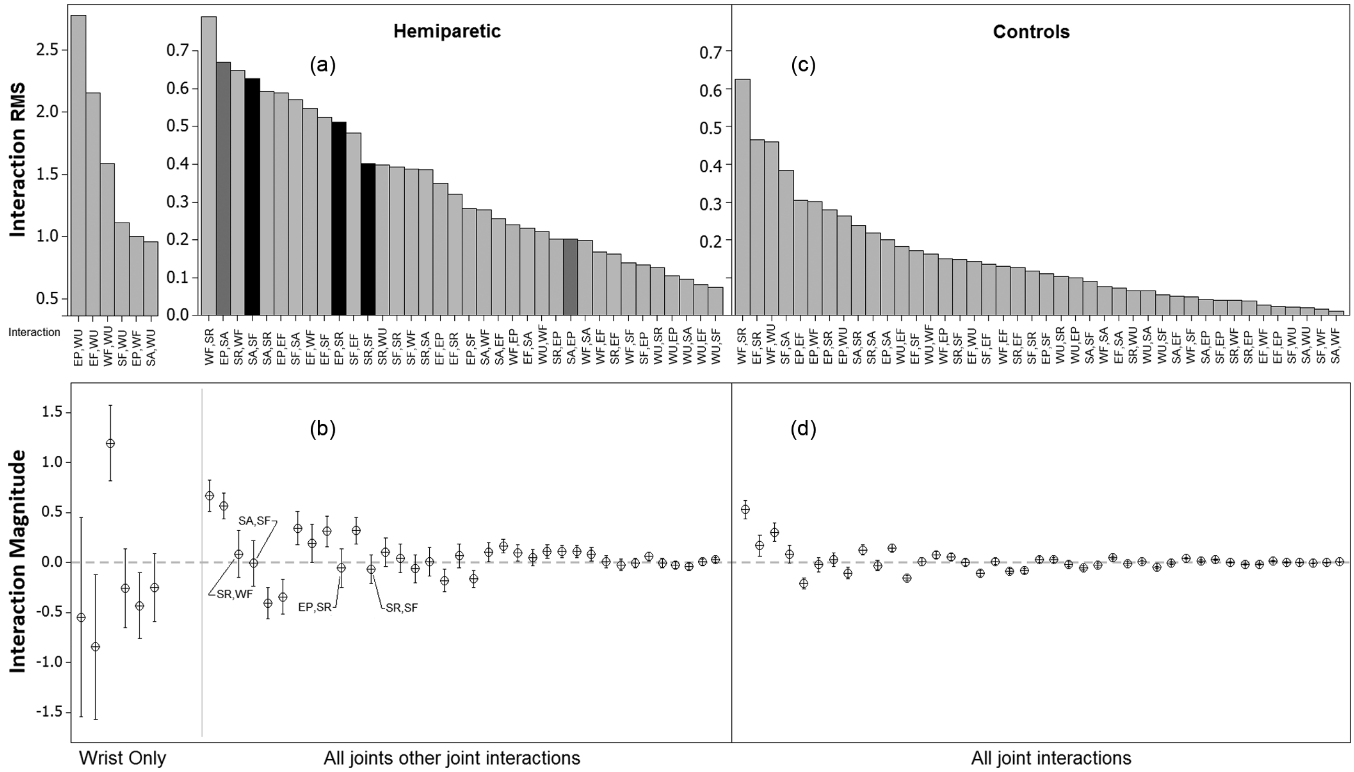

Fig. 5. Pareto chart that orders rms values in decreasing order of strengths is used in (a) and (c). Mean values and 95% CIs are given in (b) and (d). Stroke induced synergies are depicted in (a) and (b), natural synergies are depicted in (c) and (d). Dark shaded bars are referenced in the discussion.

sometimes refers to synergistic symmetry in another context [5], [22]. For the purposes of this paper, the term "symmetry" refers to whether or not the synergy matrix is symmetric. Formally, a matrix is asymmetric if interaction $(i,j) \neq (j,i)$ for $i \neq j$. An example of asymmetry is evident from the dark shaded bars in Fig. 5(a). If the matrices were typically symmetric, $(\mathrm{EP},\mathrm{SA}) \approx (\mathrm{SA},\mathrm{EP})$. However, interaction (EP, SA) is roughly three times greater than (SA, EP).

Wrist input responses accounted for a large share of variation for hemiparetic interactions. This variability is related to limited range-of-motion (ROM) in the wrist. To take an example, the matrix rms values for Subjects 2 and 4 are compared against Subjects 10 and 11. The amount of variation for subjects is expressed by calculating 95% CIs for the subjects' matrix rms values. Subjects 10 and 11 had especially large amounts of variation. Accordingly, the size of the CIs for Subjects 10 and 11 were 2.27 and 2.61 respectively while Subjects 2 and 4 had comparatively small CIs of 0.10 and 0.09. Additionally, the wrist flexion ROM in Subjects 10 and 11 ranged from 2° to 5° versus 49° to 60° for subjects 2 and 4. As subjects with limited ROM strained to move their wrist they often perturbed other joints. Given a small wrist rotation, any response rotation, regardless of how small, will result in a comparatively large calculated interaction. Due to limited wrist ROM, wrist input responses for many hemiparetic subjects were unreliable. High wrist input variability also inflated the rms calculations. The matrix rms values in Fig. 4 include wrist input interactions. Because these interactions can inflate the overall calculated synergy, the interaction comparison in Fig. 5 gives a more accurate picture. Accordingly, the left portion of Fig. 5(a) shows exaggerated interactions for wrist inputs. Recall that that the matrix rms calculations of synergy were significantly greater for hemiparetic subjects than for both control groups. Matrix rms values were recalculated with WF and WU inputs excluded. A two-sample t-test was then calculated to compare hemiparetic subjects against control subjects (age-matched and nonage-matched controls together). The hypothesis test resulted in a p-value <0.001. Therefore, even after correcting for the wrist, the hemiparetic group still has significantly larger synergy.

E. Singular Value Decomposition of the Synergy Matrix

As was mentioned earlier, singular values provide an alternative synergy measure. Previously, synergy was summarized by taking the rms of off-diagonal matrix elements, or by taking the rms for a specific interaction across subjects. However, such an approach ignores the magnitude, sign, and position of those elements within their respective matrices. As is shown by example, SVD allows for an assessment of maximum and minimum synergy in a way that factors in the *combined* effects from each joint. To demonstrate this using an example, an SVD from hemiparetic Subject 2's synergy matrix is considered. As was described previously, right singular vectors $\mathbf{v_1}$ and $\mathbf{v_7}$ are obtained from Subject 2's $\mathbf{V}$ matrix. The predicted response of Subject 2 making an intended rotation that is proportional to either $\mathbf{v_1}$ or $\mathbf{v_7}$ are depicted graphically in Fig. 6. The unshaded bars of Fig. 6 correspond to the vector elements of intended rotation (input). The shaded bars correspond to the vector of the synergistic response (output). As a reminder, the magnitudes $\|\mathbf{v_1}\|$ and $\|\mathbf{v_7}\|$ are unity by definition. Notice that the output components are mostly larger in Fig. 6(a) than in Fig. 6(b)

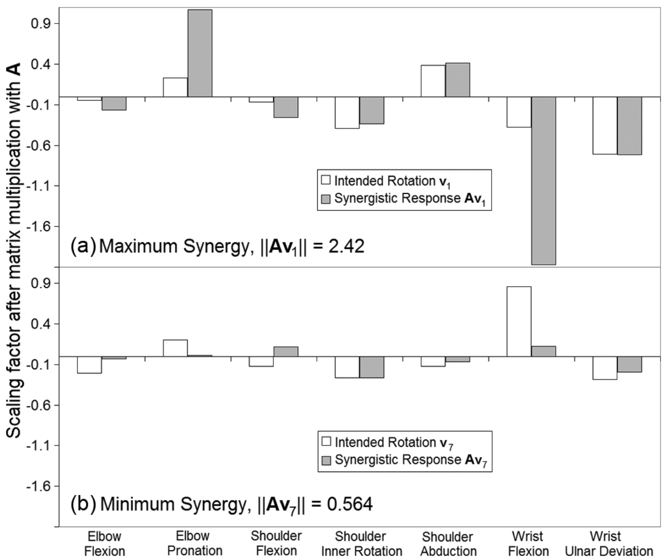

Fig. 6. Maximum and minimum synergies are depicted graphically for hemiparetic Subject 2. White bars depict intended rotation. Shaded bars depict the predicted rotation for the arm moving in synergy. Notice that the responses are mostly amplified in (a) and attenuated in (b). Because these bars relate to a liner model, the bar heights can be thought of as scaling factors.

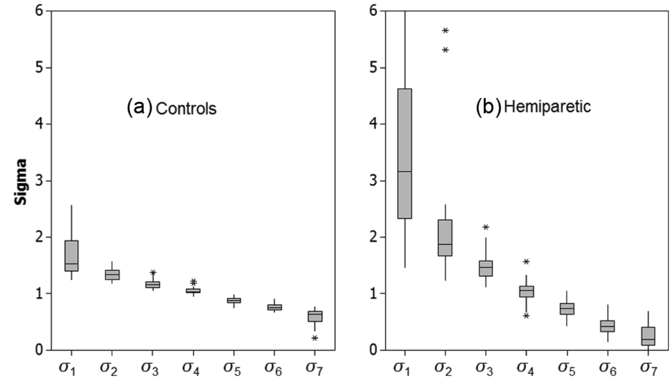

Fig. 7. Boxplots of singular values for all synergy matrices across controls and hemiparetic subjects. Asterisks depict outliers. Whiskers indicate the data ranges. The bottom of each box represents the first quartile of data, the middle line is the median, and the top of each box is the third quartile. Two σ_1 outliers at 8.6 and 8.7 in (b) are out of the graph bounds. Singular values relate to the severity of a subject's synergy.

even though the magnitudes of the input vectors are both unity. As this example demonstrates, the model predicts that when a hemiparetic individual attempts to move their arm with a combination of joints that are proportional to $\mathbf{v}_1$, the overall arm movement is exaggerated and the arm moves with maximum synergy. Conversely, when the individual attempts to move their joints in a way that is proportional to $\mathbf{v}_7$, the overall arm movement is slight and the arm moves with minimum synergy. Importantly, minimum synergy does not imply that the effects of synergy are reduced. If the effects of synergy were small then the shaded and unshaded bars would be the same. Rather, minimum synergy suggests that the overall arm movement is reduced.

Observe in Fig. 6(a) that the intended movements were mostly smaller than the predicted movements for maximum synergy. In Fig. 6(b) the intended movements were mostly larger than the predicted movement for minimum synergy. The reason that inputs proportional to $\mathbf{v}_1$ result in larger outputs than for $\mathbf{v}_7$ is because each vector in $\mathbf{V}$ is scaled by a singular values in $\mathbf{\Sigma}$. The singular values are ordered in ascending order along the diagonal of $\mathbf{\Sigma}$, therefore, $\|\mathbf{Av}_1\| \geq \|\mathbf{Av}_2\| \geq \|\mathbf{Av}_3\| \geq \|\mathbf{Av}_4\| \geq \|\mathbf{Av}_5\| \geq \|\mathbf{Av}_6\| \geq \|\mathbf{Av}_7\|$. Singular values, σ_j, were calculated for every interaction according to (4). Boxplots of singular values for all subjects are depicted in Fig. 7. A one-way ANOVA was performed on the singular values for controls, and then for stroke survivors. For both ANOVAs the singular values were significantly different with p-values <0.001. More importantly, hemiparetic singular values were more extreme than controls. For controls, the median of the largest singular values was 2.4 times larger than the median of the smallest singular values. However, it was 16.9 times larger for hemiparetic subjects. This suggests that the minimum and maximum scaling exemplified in Fig. 6 are more severe for stroke survivors than for neurologically intact individuals.

Importantly, the SVD results depicted in Fig. 6 and 7 are being used to interpret these data in a different way than is often done. As was discussed in the Methods section, SVD is often used to simplify the matrix, i.e., reduce its rank. However, in this context it is used to evaluate specific intended joint combinations. In particular, it is being used to evaluate joint combinations that are proportional to the right singular vectors. One way to visualize right singular vectors, $\mathbf{v}_1$ and $\mathbf{v}_7$, are as worst-case selections of intended joint movement. Thus, $\mathbf{v}_1$ results in the most exaggerated movement and $\mathbf{v}_7$ results in the most restricted movement. Notice in Fig. 6(a) that the synergistic rotations are mostly larger than the intended rotations. This was anticipated because the largest singular value, σ_1, was relatively large. An even larger singular value would translate to an even larger synergistic response. Conversely, the synergistic rotations in Fig. 6(b) are mostly smaller than the intended rotations. If the smallest singular value, σ_7, were even smaller, this would translate to an even smaller synergistic response.

For the ideal case, the effects of synergy are small and the magnitudes of the synergistic rotations are approximately the same as the magnitude of intended rotations. In that case, the singular values would all approximately equal one. Notwithstanding, performing SVD on the identity matrix (zero synergy) results in singular values that are all equal to 1. Because maximum and minimum synergies are undefined for zero synergy, if σ_1 or σ_7 are equal to 1, then maximum and minimum synergy are likewise undefined. Accordingly, the narrower range of singular values in Fig. 7(a) as compared to Fig. 7(b) imply that the synergistic rotations will more closely match intended rotations for controls than for hemiparetic subjects.

IV. Discussion

The interactions were nonunique to varying extents in that the synergistic paths were sometimes different for flexion than extension. If the interactions were nonlinear, and the flexion-extension paths followed along the same curve, then a unique, nonlinear function could still describe the interaction. However, this is not the case for Fig. 3(c). If interactions were nonlinear and they follow one curve in flexion, and another curve in extension, then separate nonlinear functions are needed to describe both directions. A more complicated model such as this would better explain Fig. 3(c). An alternative hypothesis for nonuniqueness is that there exists a time advance (i.e., phase lead), or time delay (i.e., phase lag) of the joint rotating in synergy relative to the joint being intentionally rotated. If joint "A" begins to rotate slightly before joint "B," and joint A also stops rotating slightly before joint B, the resulting path on an angle-angle plot of A versus B will be curved. If joint A rotates in flexion, and then extends back to its start position, a delayed response for joint B will result in a path that forms a loop on an angle-angle plot. Such leads or lags would explain the differing flexion and extension paths on plots such as Fig. 3(c). If phase leads and lags are responsible for nonuniqueness then a more complete model that accounts for phase might require complex functions, or possibly parametric equations.

From a clinical perspective, synergy is typically described in observational terms without specifics about the patient's intended joint rotations, i.e., vector $\mathbf{x}$ in (3). Accordingly, the difference between intended and actual movement is vaguely described as being "evoked as an associate reaction and performed semivoluntarily" [5]. In this way, assessments of synergy that involve multi-joint arm movements are problematic in that the specific synergistic contributions from each joint are confounded. An example of confounded observations is provided by the interaction (WF, SR), i.e., wrist flexion as an involuntary response to shoulder inner rotation. This was the strongest interaction for both hemiparetic and control subjects [see Fig. 5(a)]. Interestingly, wrist flexion is typically described as a flexor synergy while shoulder inner rotation is typically described as an extensor synergy. Thus, the classical definition of flexor and extensor synergies does not fully describe specific interactions such as this. Such a discrepancy is explainable by the model. The interactions (WF, EF), (WF, SA), and (WF, WU) were consistent with the classical flexor description. Thus, the contribution of (WF, EF), (WF, SA), and (WF, WU) may overwhelm the contribution of (WF, SR). In other words, though the wrist may appear to flex while the shoulder externally rotates for multi-joint movements, the cause for the flexion could result from the combined contribution of the other joints and not necessarily from the single contribution of shoulder external rotation. In that respect other joints confound the observation.

Though most interactions were consistent with the stereotypical description of synergy, there were some exceptions. In particular, (EP, SA) and (WF, SR) were the two strongest synergies not involving the wrist as an input. These synergies were also in violation of the flexor-extensor synergies. From the start position, both synergies involve rotation of joints along parallel axes. For example, (EP, SA) involve rotation along axes that are parallel to the coronal plane. A task that matches this synergy would include turning a doorknob clockwise with the left hand. Such a task requires a combination of wrist pronation and shoulder abduction, (EP, SA). The interaction (WF, SR) involves rotation along axes parallel to the transverse plane. A task that matches this synergy would include swinging a door open after the knob was turned. Such a task requires a combination of shoulder inner rotation and wrist flexion, (WF, SR). All hemiparetic subjects were in their chronic phase of recovery. Though learned nonuse of the paretic arm is a known problem for stroke survivors [24], subjects may have used their paretic arm to perform tasks associated with ADL, such as moving or twisting objects. Therefore, a possible explanation for violations of flexor-extensor synergies is that they relate to learned tasks that predominantly involve combination of two joints. In this way, hemiparetic subjects might have overcome, or even reversed their synergies for certain interactions through ADL.

A minority of interactions differed significantly from subject to subject. Another consideration is that the observations that were used to define flexor and extensor synergies might have been flawed due to the confounding use of multi-joint arm movements. For these reasons, a stereotypical description that divides synergy into two broad groups, flexor and extensor, should be regarded as a generalization and that individual exceptions are likely to exist.

Matrix asymmetry could have therapeutic implications. For example, the synergistic response of elbow pronation due to shoulder abduction (EP, SA) was much greater than the synergistic response of shoulder abduction due to elbow pronation (SA, EP). Therefore, if a therapist wanted to reduce synergy between these joint axes, it might be more beneficial to target intentional shoulder abduction movements rather than elbow pronation movements.

As an alternative to evaluating specific interactions, SVD provides a quantitative alternative for multi-joint arm movements. The ranges of singular values for hemiparetic subjects were larger than controls. As a hemiparetic arm moves, it will have exaggerated movement for some joint combinations, and apparent lack of movement for other joint combinations [12]. In other words, synergies could combine in a way to exaggerate joint movement when interactions combine (maximum synergy), and limit joint movements when interactions compete (minimum synergy). Practically speaking, hemiparetic arm movements may appear jerky, or have configurations in which the arm appears to stall. A therapist might attribute this to weakness, limited ROM, or spasticity. In reality, such motions might in fact result from the competing effects of joint synergy. These considerations could play a role for more precise clinical diagnoses and assessment of joint synergies.

While it is true that exaggerated, unintended movement is an importation aspect of motor dysfunction, so to is lack of movement. The therapeutic community often describes synergy in terms of maximum synergy. However, it was shown quantitatively that synergy might also impede voluntary motion through minimum synergy. Interestingly, minimum synergy most severely restricts voluntary movement when the minimum singular values are especially small. The importance of small singular values is in contradiction to the way singular values are typically treated in other applications of SVD. For example, in signal processing, smaller singular values are discarded as a way to reduce noise. For digital image compression, they are discarded in order eliminate data that has a small contribution to image quality. In statistics they are discarded as a way to reduce variation (PCA). In all cases, the smaller a singular value is, the more likely it is to be discarded. However, in terms of the synergy matrix, small singular values are potentially just as important as large ones.

V. Conclusion

The findings from this study provide a quantitative basis for defining, assessing and targeting treatment of synergies in patients post stroke. Given that hemiparetic synergy reduction is a therapeutic goal, these findings provide a quantitative basis with which to define, assess, and target synergies. Furthermore, these findings show that multi-joint synergy assessments might obscure, or confound the therapist's evaluation. Even though a motion capture system was used to measure synergy in this work, it is feasible that a therapist could assess synergy through visual inspection under a similar protocol. The results of this study provide support for clinical practice guidelines in stroke and head injury rehabilitation. Occupational and physical therapists should instruct patients to selectively and voluntarily move affected extremities and joints without engaging abnormal synergistic patterns of movement.

The proposed modeling approach for joint synergy may facilitate new types of control algorithms for use in robotic physical therapy. Such control algorithms may enable continuous monitoring of rehabilitation progress by tracking synergy reduction in stroke survivors [25], [26]. Additionally, it might allow for new types of therapy whereby the robot adjusts movement training and/or visual feedback in ways that targets a patient's individual synergies [21], [27].

Finally, this modeling approach might have practical applications for use with lower-cost motion capture systems as they become increasingly available and affordable. Physical therapists can translate the findings from this kinematic study to practice by integrating over the counter games for assessment and physical therapy treatment. This could be accomplished with the Kinect (Microsoft, Redmond WA, USA), and the Playstation Eye (Sony, Tokyo, Japan) because both systems use a camera system for movement detection. Patients could not only be instructed to use selective voluntary movement pattern to play the game but also to avoid abnormal synergistic movements during game playing. Therapists could also objectively document voluntary movement performance capabilities before and after training. Further, patients could use the gaming technology for home training.

Acknowledgment

The authors would like to thank all of the stroke survivors for their altruistic participation. Also appreciated is the advice and training provided by Dr. N. Byl of UCSF. Finally, the contributions of Z. Wells, and C. Yoo, as well as many undergraduates in the UCSC Bionics Lab are recognized. These individuals were indispensable in gathering and processing the sizable data set associated with this work.

References

[1] *Circulation* vol. 125, no. 1, pp. e2–e2220, 2012 [Online]. Available: http://cic.ahajounals.cor/content/125/1/e2.short

[2] S. Balasubramanian, R. Wei, R. Herman, and J. He, "Robot-measured performance metrics in stroke rehabilitation," in *Proc. Complex Med. Eng. Conf.*, New York, 2009, pp. 1–6.

[3] S. Kautz, S. A. Brown, and D. A. , "Relationship between timing of muscle excitation and impaired motor performance during cyclical lower extremity movement in post-stroke hemiplegia," *Brain*, vol. 121, no. 3, pp. 512–526, 1998.

[4] M. Tresch and A. Jarc, "The case for and against muscle synergies," *Current Opin. Neurobiol.*, vol. 19, no. 6, pp. 601–607, 2009.

[5] S. Brunnstrom, *Movement Therapy in Hemiplegia: A Neurophysiological Approach*. New York: Harper Row, 1970, pp. 7–14.

[6] P. W. Duncan, M. Propst, and S. G. Nelson, "Reliability of the Fugl-Meyer assessment of sensorimotor recovery following cerebrovascular accident," *Phys. Ther.*, vol. 63, no. 10, pp. 1606–1610, 1983.

[7] J. Dewald, V. Sheshadri, M. Dawson, and R. Beer, "Upper-limb discoordination in hemiparetic stroke: Implications for neurorehabilitation," *Top Stroke Rehabil.*, vol. 8, no. 1, pp. 1–12, 2001.

[8] S. Sangani, A. Starsky, J. McGuire, and B. Schmit, "Multijoint reflex response to constant-velocity movements of the stroke elbow," *Neurophysiology*, vol. 102, no. 3, pp. 1398–1410, 2009.

[9] J. Dewald, P. Pope, J. Given, T. Buchanan, and W. Rymer, "Abnormal muscle co-activation patterns during isometric torque generation at the elbow and shoulder in hemiparetic subjects," *Brain*, vol. 118, no. 2, pp. 495–510, 1995.

[10] J. Dewald and R. Beer, "Abnormal joint torque patterns in the paretic upper limb of subjects with hemiparesis," *Muscle Nerve*, vol. 24, no. 2, pp. 273–283, 2001.

[11] S. Kautz and D. Brown, "Relationships between timing of muscle excitation and impaired motor performance during cyclical lower extremity movement in post-stroke hemiplegia," *Brain*, vol. 121, no. 2, pp. 515–526, 1998.

[12] R. D. Trumbower, V. J. Ravichandran, M. A. Krutky, and E. J. Perreault, "Contributions of altered stretch reflex coordination to arm impairments following stroke," *J. Neurophysiol.*, vol. 104, no. 6, pp. 3612–3624, 2010.

[13] D. Reisman and J. Sholz, "Aspects of joint coordination are preserved during pointing in persons with post-stroke hemiparesis," *Brain*, vol. 126, no. 11, pp. 2510–2527, 2003.

[14] M. Cirstea and M. Levin, "Compensatory strategies for reaching in stroke," *Brain*, vol. 123, no. 5, pp. 940–953, 2000.

[15] L. Dipietro, H. Krebs, S. Fasoli, B. Volpe, J. Stein, C. Bever, and N. Hogan, "Changing motor synergies in chronic stroke," *J. Neurophysiol.*, vol. 98, no. 2, pp. 757–768, 2007.

[16] J. J. Craig, *Introduction to Robotics*. Upper Saddle River, NJ: Pearson Prentice Hall, 2005, p. 241.

[17] L. Stark, M. Iida, and P. Willis, "Dynamic characteristics of the motor coordination system in man," *Biophys. J.*, vol. 1, pp. 279–300, 1961.

[18] M. C. Cirstea, M. C. Levin, and M. F. , "Compensatory strategies for reaching in stroke," *Brain*, vol. 123, no. 5, pp. 940–953, 2000.

[19] P. Archambault, P. Pigeon, A. Feldman, and M. Levin, "Recruitment and sequencing of different degrees of freedom during pointing movements involving the trunk in healthy and hemiparetic subjects," *Exp. Brain Res.*, vol. 126, no. 1, pp. 55–67, 1999.

[20] T. Bockemuhl, N. F. Troje, and V. Durr, "Inter-joint coupling and joint angle synergies of human catching movements," *Human Movement Sci.*, vol. 29, no. 1, pp. 73–79, 2010.

[21] C. Crocher, A. Sahbani, J. Robertson, A. Roby-Brami, and G. Morel, "Constraining upper limb synergies of hemiparetic patients using robotic exoskeleton in the perspective of neuro-rehabilitation," *IEEE Trans. Neural Syst. Rehabil. Eng.*, vol. 20, no. 3, pp. 247–257, May 2012.

[22] G. Strang, *Introduction to Linear Algebra*. Wellesley, MA: Wellesley-Cambridge Press, 1998, pp. 113–317.

[23] S. Boyd, Lectures on the applications of singular value decomposition in LDS and electrical engineering Jul. 8, 2008 [Online]. Available: http://www.stanford.edu/~boyd/ee263/videos.html

[24] J. Liepert, W. H. R. Miltner, H. Bauder, M. Sommer, C. Dettmers, E. Taub, and C. Weiller, "Motor cortex plasticity during constraint-induced movement therapy in stroke patients," *Neurosci. Lett.*, no. 250, pp. 5–8, 1998.

[25] P. Lum, C. Burgar, M. Van der Loos, P. Shor, M. Majmundar, and R. Yap, "MIME robotic device for upper-limb neurorehabilitation in subacute stroke subjects: A follow-up study," *J. Rehabil. Res. Develop.*, vol. 43, no. 5, pp. 631–642, 2006.

[26] A. Al-Refai, M. Simkins, N. Byl, and J. Rosen, Objectively characterized linear model of stroke induced joint synergy in relation to clinical measures, unpublished.

[27] G. Alankus, A. Laza, M. May, and C. Kelleher, "Towards customizable games for stroke rehabilitation," in *Proc. CHI 2010*, Apr. 10–15, 2010, pp. 2113–2122.

Matt Simkins was born in San Jose, CA, USA, in 1975. He received the B.S. degree in mechatronics engineering from Chico State, Chico, CA, USA, in 2004. He is currently working toward the Ph.D. degree at the University of California at Santa Cruz, Santa, Cruz, CA, USA.

His current work includes robotically assisted movement training, characterizations of joint synergies, and human motor learning. He has a Six Sigma Black Belt and has helped to launch dozens of products in the medical device and pharmaceutical industries from 2004 to 2009. Prior to that he worked as an electronics consultant. He is the owner of a company that designs and manufactures sports equipment.

Aimen H. Al-Refai (M'10) received the BFA degree in graphic arts from University of Missouri at Warrensburg, Warrensburg, MO, USA, in 1989, and the M.S. degree in computer engineering—robotics and controls from University of California at Santa Cruz, Santa Cruz, CA, USA, in 2012.

He currently works as an Embedded Systems Engineer at Broadband Discovery Systems. He has worked for Apple in quality assurance and as a software engineer with Sesame Technologies, Disney, and Infoseek. Prior to that he worked as a graphic designer for 12 years working on various projects such as wine labels to physic and chemistry text books.

Jacob Rosen (M'01) received the B.Sc. degree in mechanical engineering and the M.Sc. and Ph.D. degrees in biomedical engineering from Tel-Aviv University, Tel-Aviv, Israel, in 1987, 1993, and 1997, respectively.

From 1993 to 1997, he was a Research Associate developing and studying the myosignal-based exoskeleton at the Biomechanics Laboratory, Tel-Aviv University. From 1997 to 2008, he was at the University of Washington as an Associate Professor of Electrical Engineering. Since 2008 he has been an Associate Professor at the University of California at Santa Cruz, Santa Cruz, CA, USA. His research focus is surgical robotics, wearable robotics, biomechanics, and human-machine interface.